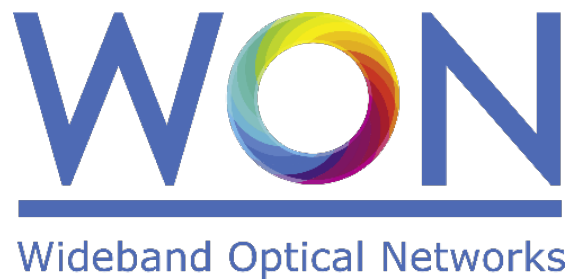


Marie Skłodowska-Curie (MSCA) – Innovative Training Networks (ITN)  
H2020-MSCA-ITN European Training Networks



## Wideband Optical Networks [WON]

Grant agreement ID: 814276

**WP3 – [In-line component design]**

**D3.2 – [Design of Raman and Bi-doped amplifier]**



*This project has received funding from the European Union's Horizon 2020 research and innovation programme under the Marie Skłodowska-Curie grant agreement 814276.*

## Document Details

Work Package	WP3- In-line component design
Deliverable number	D3.2
Deliverable Title	Design of Raman and Bi-doped amplifier
Lead Beneficiary:	Aston University
Deliverable due date:	31 December 2020
Actual delivery date:	1 June 2021
Dissemination level:	Public

## Project Details

Project Acronym	WON
Project Title	Wideband Optical Networks
Call Identifier	H2020-MSCA-2018 Innovative Training Networks
Coordinated by	Aston University, UK
Start of the Project	1 January 2019
Project Duration	48 months
WON website:	<a href="https://won.astonphotonics.uk/">https://won.astonphotonics.uk/</a>
CORDIS Link	<a href="https://cordis.europa.eu/project/rcn/218205/en">https://cordis.europa.eu/project/rcn/218205/en</a>

## WON Consortium and Acronyms

Consortium member	Legal Entity Short Name
Aston University	Aston
Danmarks Tekniske Universitet	DTU
VPIphotonics GmbH	VPI
Infinera Portugal	INF PT
Fraunhofer HHI	HHI
Politecnico di Torino	POLITO
Technische Universiteit Eindhoven	TUE
Universiteit Gent	UG
Keysight Technologies	Keysight
Finisar Germany GmH	Finisar
Orange SA	Orange
Technische Universitaet Berlin	TUB
Instituto Superior Tecnico, University of Lisboa	IST

## Abbreviations

BDFA: Bi-doped fibre amplifier  
DCF: Dispersion compensation fibre  
DSF: Dispersion shifted fibre  
DWDM: Dense wavelength Division multiplexing  
EDFA: Erbium-doped fibre amplifier  
ETN: European Training Network  
HNLF: Highly non-linear fibre  
IDF: Inverse dispersion fibre  
MBT: Multi band transmission  
Nd: neodymium  
NF: Noise figure  
OSA: Optical spectrum analyser  
SDM: Spatial division multiplexing  
SMF: Single mode fibre  
TFF-WDM: Thin film filter wavelength division multiplexer  
TL: Tunable lasers  
WDM: Wavelength Division multiplexing

## Table of Contents

EXECUTIVE SUMMARY .....	5
1. INTRODUCTION .....	6
2. OVERVIEW RAMAN AMPLIFIER .....	8
3. RAMAN AMPLIFIER CONFIGURATION.....	9
3.1 Distributed Raman amplifier .....	9
3.2 Pumping schemes in Raman amplifiers .....	10
3.3 Wideband Raman amplifiers .....	10
3.4 Results and Discussion .....	11
3.5 Conclusion .....	12
4. BISMUTH-DOPED FIBRE AMPLIFIER .....	13
4.1 Types of bismuth-doped fibres .....	13
4.2 Developed Bi-doped fibre amplifier .....	14
4.3 Conclusion .....	17
REFERENCES .....	18

## EXECUTIVE SUMMARY

The present scientific deliverable is a part of the Work Package 3 “Inline component design” of ETN project WON “Wideband Optical Network”, funded under the Horizon 2020 Marie Skłodowska-Curie scheme Grant Agreement 814276

The document presents an overview of Raman and Bismuth doped amplifiers that are potential candidates for wideband signal amplification. In terms of Raman amplification, the system design involves integration of suitable gain fibre which is inverse dispersion fibre in our case in accordance to past literature review and laser diodes extending from 1325 nm to 1508 nm. The target signal amplification is within the spectral range of 1410 nm -1625 nm (~ 215 nm bandwidth) with flat signal gain and optimized noise figure. The amplifier design is based on a multistage split combine approach in order to avoid pump-signal and pump-pump overlap. This document describes the initial modelling results of wideband Raman amplifier in terms of gain and noise figure. In terms of the Bi-doped fibre amplifier, the target for the project is a design of Bi-doped fibre amplifier from 1310 to 1510 nm in a multi-stage or single-stage configuration. As the first step, a single-stage Bi-doped fibre amplifier with maximum gain of 32 dB, and minimum NF of 4.75 dB was designed, constructed and demonstrated in a spectral band of 1405-1460 nm.

## 1. INTRODUCTION

Transmission distance of any fibre-optic communication system is eventually limited by the level of fibre loss. Until 1995, this loss limitation was overcome using optoelectronic repeaters. These devices convert optical signals into electric form using the receiver, and then convert this signal back to the optical representation in the transmitter. These regenerators became very complex and expensive, as they required high repeating speed and demultiplexing in the wide spectral band [1]. An alternative for sophisticated optoelectronic repeaters are optical amplifiers, which amplify each signal wavelength without converting them into electric signal [1]. The majority of the optical amplifiers were invented in the 1980s, and in the 1990s they started to be implemented in the first light wave systems.

Nowadays optical amplifiers are the inherent parts of optical telecom systems. The most widely spread type of amplifier is the Erbium-doped fibre amplifier (EDFA) that is capable of covering C- and L- optical telecommunication spectral bands. With the help of coherent optical technologies contemporaneous telecom systems support up to 38.4Tb/s/fibre [2]. However, the last two decades showed exponential growth of demand on internet traffic speed, which is expected to be ceaseless in the future. Thus, this large speed might be insufficient for future internet traffic demand. Moreover, currently the deployment of 5G networks, fast development of cloud services, and increased amount of information required for transmission in machine-to-machine communication, should further load the existing telecommunication infrastructure. Three different approaches were proposed to cope with ceaseless increase of speed requirements: spatial division multiplexing (SDM) with multi-fibre or multi-core/mode fibre transmission; implement new coding modulation formats with high spectral efficiency; and multi band transmission (MBT) using single fibre [3]. The SDM implementation through multi-fibre transmission leads to increased cost of optical telecom systems because of demand on new fibre rolling out [2]. On the other hand, use of multi-core/mode fibres for the transmission lead to potential capacity of Petabit/s/fibre [4, 5], though the technology of such transmission is too immature to be used for commercial use. According to the current state-of-art on spectral efficient modulation formats, the Shannon limit in terms of spectral efficiency is close to be achieved. The efforts to increase signal-to-noise-ratio and allow wide use of complex modulation formats through low-noise optical amplification, lower-loss and lower-nonlinearity fibres, or digital nonlinear compensation [6] yields only logarithmic increase, which can allow traffic growth only on the short-term basis. As the commercial systems are close to Shannon limit in terms of spectral efficiency within C-band, operators aim to maximize the return-on-investments on existing infrastructures [7]. From this perspective, MBT is an attractive solution, as it postpones new fibre rollouts, and it aims on transmission in new spectral bands beyond C- band.

The first commercial MBT systems already coming to the market targeting transmission in C+L-band systems based on Erbium-doped fibre amplifiers (EDFAs). Operation in the L-band adds 60 nm to the conventional 35 nm C-band. As the next step, it is natural to continue bandwidth expansion into the next closest band that is S-band. However, the transmission in O- and E-bands should be considered as well, as they are very attractive for transmission, especially using special pure silica fibre with low loss in this spectral region [2]. However, multi-band transmission requires novel types of amplifiers for corresponding spectral bands. Many amplifier technologies were proposed to cover some or multiple bands using neodymium (Nd) [8], praseodymium (Pr) [9], or thulium <sup>TM</sup> -doped fibres [10], and Raman fibre amplifiers [11]. It was suggested already a time ago that Pr-doped as well as Nd-

doped optical fibres demonstrate emission in all the O-, E-, and S- telecom bands but suffer from the strong excited-state absorption noticeably spectrally narrowing the net gain and suppressing its magnitude [8–15]. In spite of significant recent progress achieved with a micro-structured Nd-doped silica fibre allowing suppression of the unwanted transitions through spectral filtration [12], such fibres still require further development in order to match the performance of Er-doped fibres. Since the first reports [16] Bi-doped fibre amplifiers (BDFAs) have been extensively studied as promising amplification platform for multi-band transmission [17–27]. Using different host materials such as aluminosilicate, phosphosilicate, and germanosilicate glass allows to significantly shift emission spectrum from 1150 to 1500 nm [18, 26, 27]. Bi-doped fibre amplifier with record bandwidth of 115 nm, 31 dB gain, and 4.8 dB noise figure (NF) in the O and E bands has been recently reported [27]. The first successful data transmission experiment characterised on three signal wavelengths in E-band was reported in [24] and first multi-channel amplification was reported in [23]. Moreover, the performance of Bi-doped fibre amplifier spectrally adjacent to EDFA range was studied in [26] using both backward and forward pumping schemes.

However, amplifiers based on doped fibres can support only specific target bands [28] which ultimately necessitates implementation of guard bands between corresponding spectral bands resulting in some finite bandwidth loss. Also, the segregation of amplifiers specific to each band increases the complexity and cost since, after each transmission span the corresponding spectral bands require separation followed by amplification of each target band with a suitable doped amplifier and then recombination for further transmission [28].

In contrast to doped amplifiers, Raman amplifiers can provide a solution to this shortcoming. The Raman effect is an inherent non-linear phenomenon in silica fibres [29] which can be exploited for signal amplification in any spectral region of the communication window. The characteristics of this amplifier provides a flexibility in obtaining varying gain across a large bandwidth since the gain spectrum is determined mainly by the Raman pump laser wavelengths. Using this approach, state of the art literature have already shown an extensive amplification of ~ 150 nm comprising of (S, C and L) band with 15 dB overall gain and ~ 8 dB NF with discrete Raman amplifier [30]. Also a hybrid configuration with distributed-discrete Raman has shown an amplification extending out to ~ 150 nm with an effective NF of < 0 dB for the S band signals and NF of ~ 6 dB for C and L band signals [31]. Moreover a record gain of 27 dB and average NF of 5.8 dB has been reported for C and L band optical spectrum with discrete Raman amplifier [32].

## 2. OVERVIEW RAMAN AMPLIFIER

Raman amplifier works on the principle of stimulated Raman scattering, an inherent non-linear phenomenon in which a pump photon of frequency  $\nu_p$  excites the gain material to a higher energy state, and in the process emits a photon of frequency  $\nu_s$ , as shown in Fig.1a This newly created photon contributes to a so-called Stoke's wave, which is amplified due to the transfer of energy from the pump photon. The difference in frequency ( $\nu_p - \nu_s$ ) is known as Stoke's shift and is maximum at  $\sim 13.2$  THz (100 nm) from the pump frequency [29]

Fig. 1b shows the Raman gain spectrum profile for pump at 1445 nm wavelength. The maximum peak gain occurs at  $\sim 100$  nm shift from the pump wavelength. Figure.1b also shows that the gain profile is not uniform, and thus signals lying within the gain curve undergo unequal amplification.

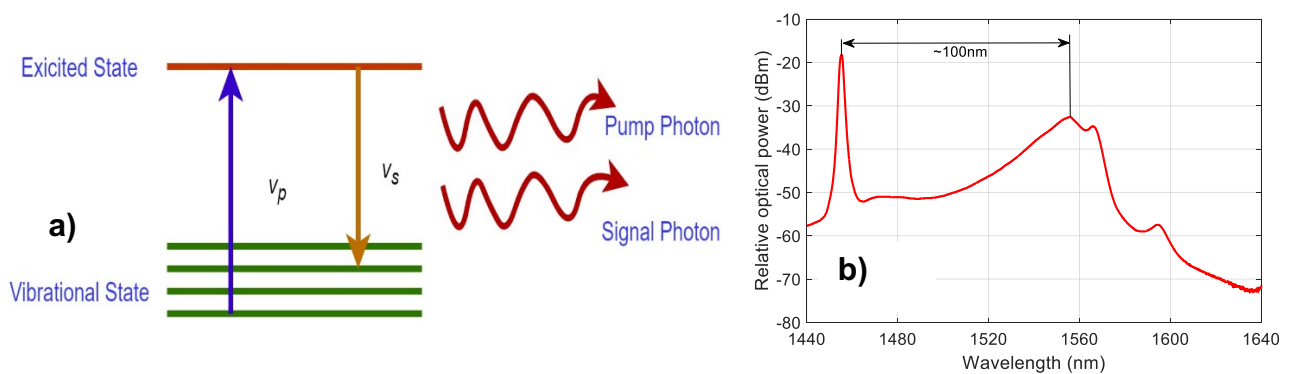


Fig. 1 a) Stimulated Raman scattering b) Raman Stoke's shift

Combination of multiple Raman Effect generated with various pumps at selective wavelength generates a broadband spectrum due to an averaging effect which can be observed from the Fig. 2 dotted magenta line. The optimization of pump powers and wavelengths a key feature in governing the gain dynamics of this amplifier and proper tuning of the pump power results in obtaining flat gain across a target bandwidth.

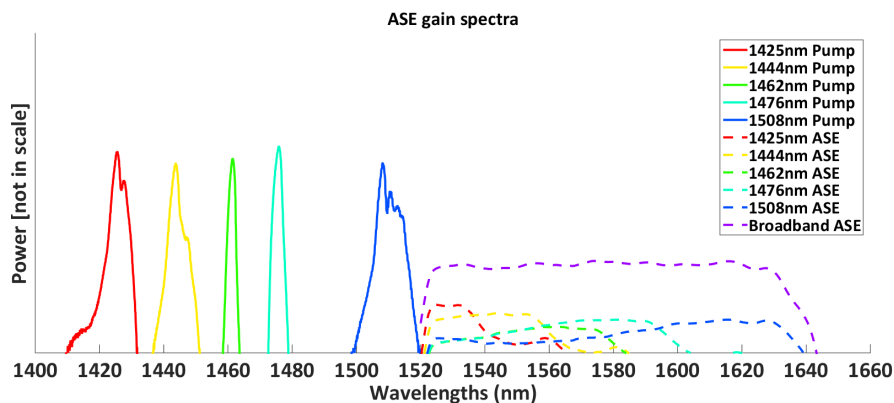


Fig. 2: Broadband ASE generation using Raman pumps



### 3. RAMAN AMPLIFIER CONFIGURATION

Raman amplifiers are mainly categorized into two types 1) Distributed Raman amplifier 2) Discrete Raman amplifier.

#### 3.1 Distributed Raman amplifier

In a distributed Raman configuration, the transmission fibre itself act as an amplifying medium and signals are amplified as they propagate along its length. As the signal propagates through the fibre it undergoes attenuation which is counterbalanced by amplification in the fibre itself. Since amplification occurs within the transmission fibre, no additional fibre is required for the amplification stage thereby reducing the amplifier cost [33].

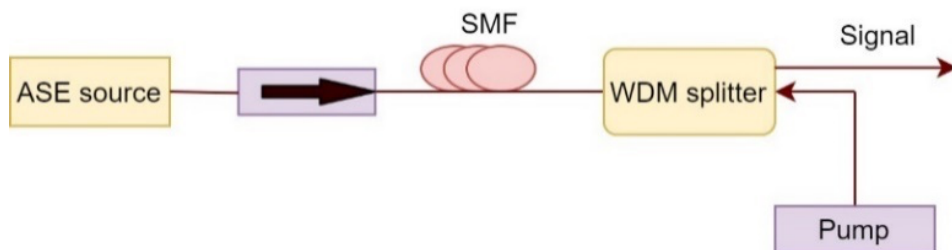


*Fig. 3: Simple schematic of backward pumped distributed Raman amplifier*

Discrete Raman amplifiers in the other hand are also known lumped amplifiers a replica of EDFAs technology. In this process amplification occurs at only certain discrete point of a gain fibre. A special fibre with high non-linearity is preferred as a gain medium. These fibres usually have high Raman gain coefficient and few kilometres of such fibres are pumped using high power lasers. There have been various developments with the advancement of fibre technology for wideband signal amplification. Reports in the literature have shown use of dispersion shifted fibre (DSF) [34], dispersion compensation fibre (DCF) [35], inverse dispersion fibre (IDF) [36] and other highly non-linear fibre (HNLF) [37] as potential gain fibre for Raman amplification in DWDM systems.

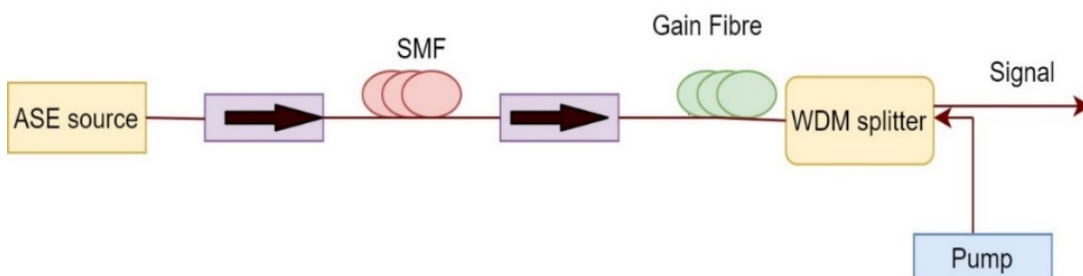


*Fig. 4 Simple schematic of backward pumped discrete Raman amplifier*

### 3.2 Pumping schemes in Raman amplifiers

There are basically three pumping schemes in Raman amplifiers,

- **Forward pumping** – Both signal and pump propagate in the same direction.
- **Backward pumping** – Pump and signal propagates in the opposite direction.
- **Bidirectional pumping** – Pump propagates both in forward and backward direction w.r.t signal

### 3.3 Wideband Raman amplifiers

Previous literature has shown a maximum gain bandwidth of 150 nm comprising S, C and L band of the communication window taking into account the impact of Rayleigh scattering due to pump signal overlapping [38]. However, there is further scope of bandwidth extension with proper optimization of pump wavelengths and powers.

In the WON project, we propose a wideband Raman amplifier with > 200 nm bandwidth comprising of the E, S, C and L bands from 1410-1625 nm of the optical spectrum. Our Raman amplifier design is based on a split and combine approach in which the transmitted signals are split down into two optical bands using a filtered WDM splitter, which are then amplified separately in dual-stages using suitable pump powers and wavelengths. These amplified bands are then recombined using a WDM combiner for further transmission as shown in Fig. 5.

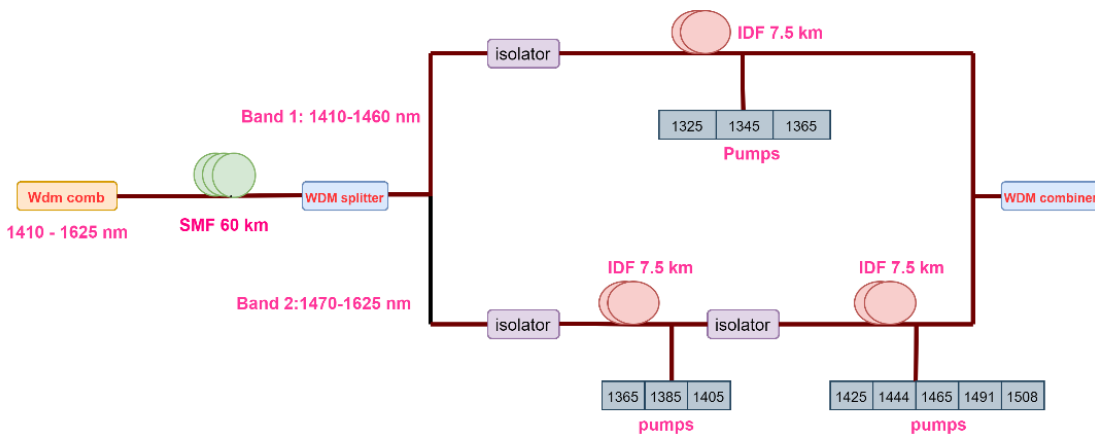


Fig. 5 Schematic of multiband discrete Raman amplifier

In broader detail, signals in the bandwidth range of 1410-1625 nm are transmitted through a standard SMF fibre. The transmitted signals are then separated into two bands, one band comprising of signals from 1410-1460 nm which are then amplified using 1325 nm, 1345 nm and 1365 nm pumps. The other band comprises of signals from 1470-1625 nm and are amplified in two separate stages. The first stage comprises of 1365 nm, 1385 nm and 1405 nm pumps to amplify signals in the S band i.e. around 1470-1515 nm. The second stage comprises of 1425 nm, 1444 nm, 1465 nm, 1491 nm and 1508 nm pumps to amplify signals from 1516 to 1625 nm i.e. the C and L bands of the optical spectrum. A discrete backward pumping scheme with inverse dispersion fibre (IDF) as the Raman

gain fibre was chosen in accordance to its low noise-figure and non-linear coefficient as compared to DCF and HNLF fibre as stated in previous literature [39].

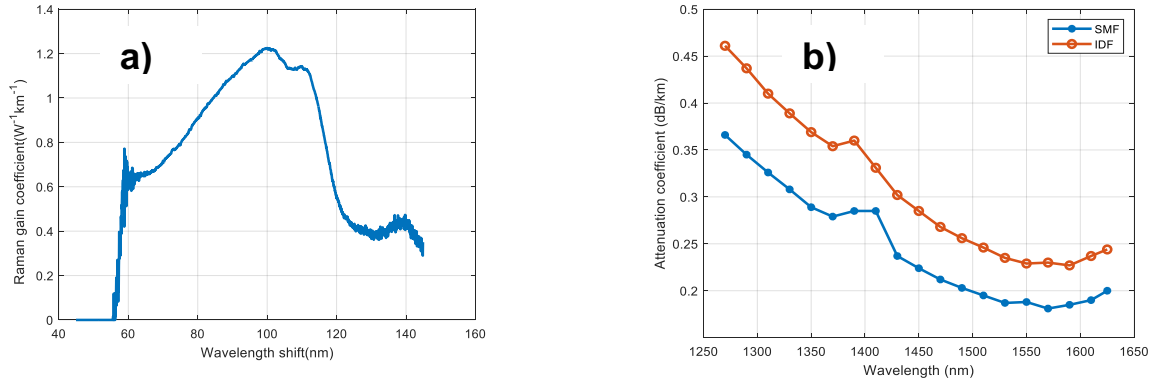


Fig. 6 a) Wavelength shift vs Raman gain coefficient for IDF fibre b) Attenuation coefficient vs wavelength for SMF and IDF fibre.

Fig. 6a shows the Raman gain coefficient of IDF and Fig. 6b shows the attenuation coefficient of IDF and SMF. Numerical modelling of Fig. 5 was carried out for 1410-1625 nm signals with VPI Transmission maker 11.0 using the split step Fourier method. An optimized step size of 50m was chosen to reduce the simulation time. The measured Raman gain coefficient and attenuation profile of IDF and SMF fibre was fitted to the wideband model to verify the performance of the simulated design. A total of 48 channels with 0 dBm power per channel was launched into the transmission fibre and the corresponding power after 50 km was noted to give an estimate of the span loss at each channel. The pump power was optimized accordingly with the obtained values from Raman optimizer of VPI Transmission maker 11.0 to mitigate the loss generated by the span attenuation and power transfer due to stimulated Raman scattering (SRS).

### 3.4 Results and Discussion

The simulated model gain, noise figure (NF) and power per channel after amplification was measured using VPI numericl-2D analyser of Photonic circuit module. Figure 7 shows the power per channel after 50 km transmission. It can be clearly seen that shorter wavelength channels have high loss after 50 km transmission as compared to longer wavelength channels. This is because of the high attenuation coefficient and inherent SRS of the shorter wavelength channels.

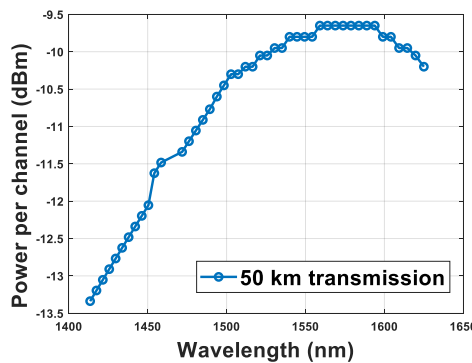


Fig. 7. Power per channel after 50 km transmission through SMF before amplifier stage

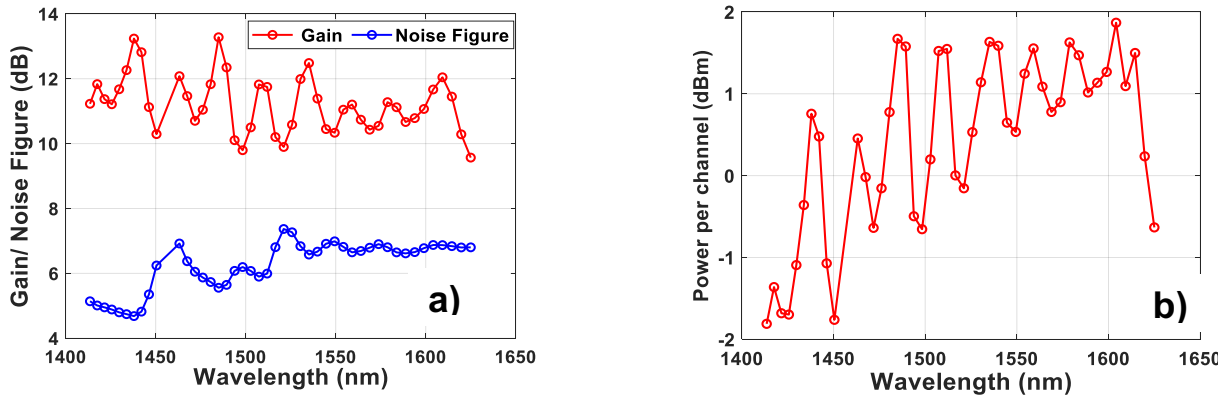


Fig. 8 a) Wavelength vs Gain/ NF b) Wavelength vs Power per channel of wideband split combine Raman amplifier

Fig. 8a shows the gain and noise figure of the simulated model. The maximum NF was observed to be 7.5 dB corresponding to higher wavelength channel with a NF tilt of a  $\sim 2$  dB for band 1 (1410-1460 nm) signals and 1.7 dB for band 2 (1470-1625) nm signals. A maximum gain of 13.5 dB was obtained by proper adjustment of pump powers to mitigate the fibre losses for the lower wavelength channels.

Fig. 8b shows the power per channel after amplification stage. Here, the maximum channel ripple was observed  $\sim 3.8$  dB without any flattening filter.

### 3.5 Conclusion

We have numerically simulated an ultra-wideband discrete Raman amplifier for wideband signal amplification. With the proposed split-combine multi-stage amplification approach, we managed to amplify signals from 1410-1625 nm i.e.  $> 200$  nm bandwidth comprising the E, S, C and L band of the optical spectrum.

The simulation results shows a maximum gain of 13.5 dB, maximum noise figure of 7.5 dB and channel ripple  $\sim 3.8$  dB over  $> 200$  nm bandwidth signals.

We believe multi stage Raman amplifier design is a promising framework for wideband signals amplification with low noise figure and optimized gain. This novel approach can be utilized for ultra-wide amplification and could play a significant role in future optical communication systems.

Further work is now underway to procure all components for this Raman amplifier design to enable experimental build and test.

## 4. BISMUTH-DOPED FIBRE AMPLIFIER

### 4.1 Types of bismuth-doped fibres

The key feature of Bi-doped fibres is that additional co-dopants shift the gain spectrum significantly. There are four main types of Bi-doped fibres with different co-dopant ions: aluminosilicate, phosphosilicate, germanosilicate, and pure silica fibres. Let us firstly consider aluminosilicate fibres. Such fibres pumped near 1  $\mu\text{m}$  absorption band have gain spectra from 1080 to 1315 nm with a maximum at 1150 nm [22]. Examples of spectral gain for different concentrations are shown in Fig. 12. The absorption of the pump in these cases were saturated, thus the achieved gain is the maximum value for the shown concentrations. The increase of the active bismuth centres concentration leads to gain decrease, along with nonsaturable absorption increase. These effects can be explained by up-conversion, excited state absorption [17]. The further increase leads to dramatic grow of passive loss in IR region [40].

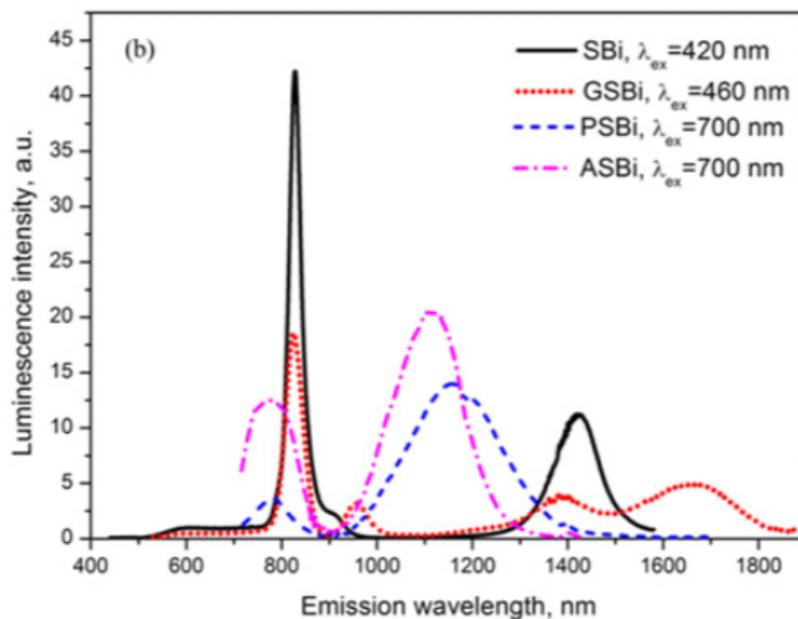


Fig.9: Small signal gain for alumina- and germanosilicate Bi-doped fibres. Figure 5: Emission spectra for four different Bi-doped fibre: SBi – pure silica Bi-doped fibre; GSBi – Germanosilicate Bi-doped fibre; PSBi – Phosphosilicate Bi-doped fibre; ASBi – aluminosilicate Bi-doped fibre. [41]

These factors strongly limit the spectral range and the magnitude of the positive net gain of Bi-doped aluminosilicate fibre amplifiers with performance in optical O-band. Another class of Bi-doped fibres is germanosilicate Bi-doped fibres. This type of fibre has strong emission spectrum in the end of E-band and in the whole S-band. The gain spectrum is partially depicted in Fig. 1. The whole spectrum for germanosilicate Bi-doped fibre is depicted in Fig. 4. The Phosphosilicate fibres have the emission spectrum slightly shifted in longer wavelength region in comparison with aluminosilicate ones [41]. On the other hand, pure-silica fibres have strong gain near 1400 nm, but have very limited spectral range. All of the above mentioned fibres have luminescence near 800 nm, but this spectral range is not of the current interest as no classical telecommunication bands lie in this part of optical spectrum.

## 4.2 Developed Bi-doped fibre amplifier

To achieve sufficient gain around 1.45  $\mu\text{m}$  the Bi-doped fibre amplifier was developed based on the Bi-doped germanosilicate fibre and was reported in [42]. The Bi-doped germanosilicate fibre used in this work was fabricated in the Dianov Fiber Optics Research Center using MCVD-solution [43]. The core of fibre consists of 95 mol%  $\text{SiO}_2$ , 5 mol%  $\text{GeO}_2$  and  $<0.01$  mol% of bismuth. The fibre core and cladding diameter are 9  $\mu\text{m}$  and 125  $\mu\text{m}$ , respectively. The numerical aperture (NA) is 0.14, and the cutoff wavelength is around 1.2  $\mu\text{m}$ . The developed Bi-doped fibre amplifier is based on a 320 m long piece of active fibre and the experimental setup for gain and NF measurements are depicted in Fig. 2.

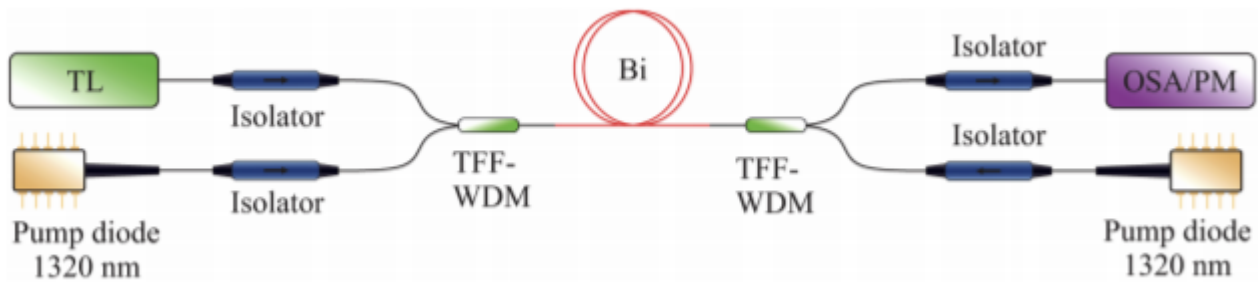


Fig. 10. Scheme of the BDFA. TL: tunable laser; TFF-WDM: thin film filter wavelength division multiplexer; Bi: Bi-doped fibre; OSA: optical spectrum analyser; PM: power meter.

Two tunable lasers (TL) operating in spectral ranges of 1340-1440 nm and 1410-1490 nm are used as a signal radiation for characterisation of the gain and NF characteristics of the developed amplifier in the spectral range of 1370-1490 nm. The first TL is used to cover spectral band up to 1440 nm, and another one in the band of 1440-1490 nm. The radiation of the TLs pass a polarisation independent isolator with minimum isolation of 32 dB and internal losses less than 3 dB in the spectral band of 1390-1490 nm. After the isolator the radiation is coupled into the Bi-doped fibre through a thin film filter wavelength division multiplexer (TFF-WDM). The key components of the developed setup are TFF-WDMs with very steep and consistent transmission (1300-1362 nm) and reflection (1370-1565 nm) bands with constant optical loss of 0.1 dB. The radiation of two pump diodes operating at the wavelength of 1320nm, used as forward and backward pumps, passes 1320 nm polarisation independent isolators and is coupled into the active fibre through TFF-WDMs. After a subsequent amplification in the Bi-doped fibre, the signal radiation passes another TFF-WDM and the 1390-1490 nm polarisation independent isolator and is detected in either optical spectrum analyser (OSA) or power-meter (PM). The OSA is used for both peak-to-peak gain measurements and the noise spectral power density subtraction for NF calculation that is found using the source subtraction technique described in [44].

The performance of the developed BDFA is characterised for the forward, backward, and bi-directional pumping schemes and three different signal levels of -20 dBm, -10 dBm, and 0 dBm. The gain and NF for the forward pumping scheme and 3 different signal levels are depicted in Fig. 11.



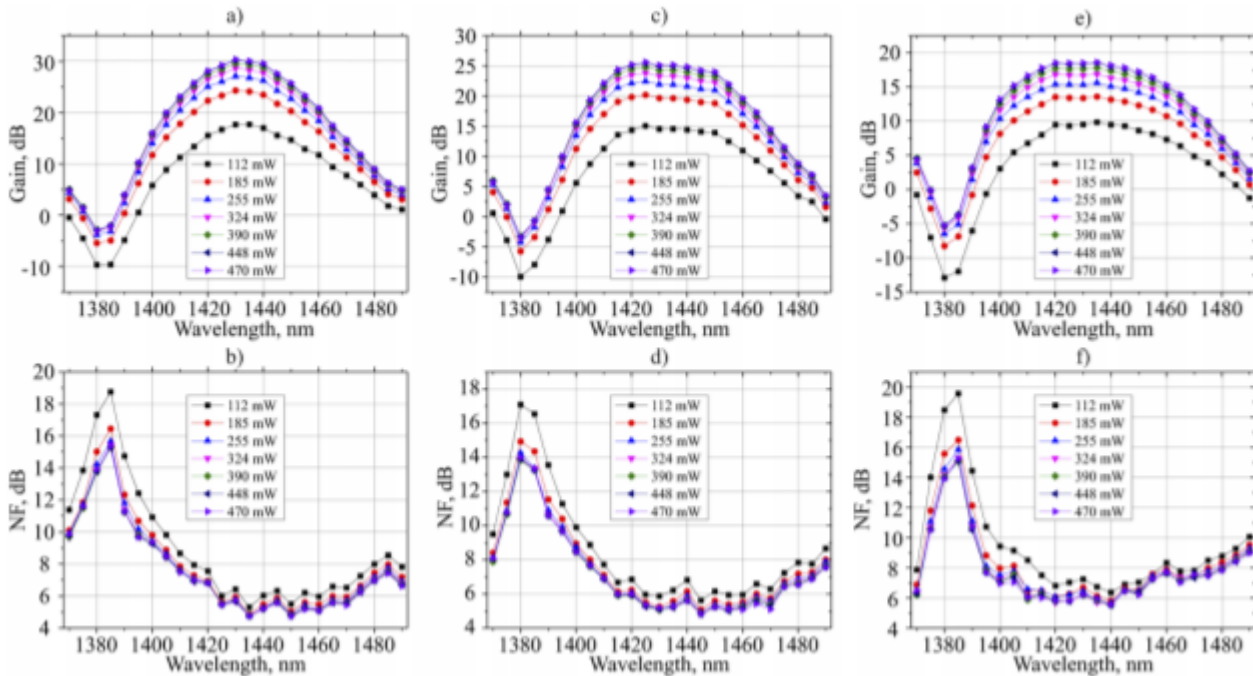


Fig. 11. Dependencies of the measured gain (upper row) and the noise figure (bottom row) on the wavelength for different pump powers in a forward pumping scheme: a,b) gain, NF for -20 dBm input signal power; c,d) gain, NF for -10 dBm input signal power; e,f) gain, NF for 0 dBm input signal power

The gain increases with the pump power increase and saturates at high pump powers for all signal power levels in Fig. 3 (a,c,e). The maximum gain of 30.36 dB is achieved at the wavelength of 1430 nm, pump power of 470 mW and signal power of -20 dBm. The gain spectrum shows a significant flattening with the increase of signal power leading to a widening of -3dB gain bandwidth from 27.28 to 52.1 nm for -20 dBm and 0 dBm signal power, respectively. Moreover, increase of the signal power leads to consistent gain reduction from maximum value of 30.36 dB to 18.63 dB for -20 dBm and 0 dBm of signal power. This effect also causes the increase of NF value from 4.75 dB to 5.56 dB.

The corresponding NF and is shown in Fig. 11 (b, d, e). The NF decreases with the increase of the pump power and saturates along with the gain saturation. The significant increase of NF closer to 1390 nm corresponds to the amplification at the edge of the gain band, the decrease of the isolator transmission, and the influence of the water absorption tail. The amplification at 1370 nm occurs due to stimulated emission from the pump level and leads to decreased NF in comparison to the signal amplification at 1390 nm. The amplification beyond the presented spectral band was not possible due to the limitations of the TFF-WDM reflection band starting from 1370 nm. The minimum NF of 4.75 dB is achieved with a - 20 dBm signal at the 1435 nm wavelength and 470 mW of pump power. All the achieved spectra from other signal powers have the similar values and the overall characteristics in terms the gain, gain bandwidth, and NF for all pumping schemes are compared in Table 1.

Signal power	Pumping scheme	Gain, db	Bandwidth, nm	NF, db
-20 dBm	forward	30.36	27.28	4.75
	backward	30.59	28.98	5.3
	bi-directional	30.52	29.08	5.26
-10 dBm	forward	25.63	42.38	4.82
	backward	26.88	38.19	5.52
	bi-directional	26.57	37.13	5.5
0 dBm	forward	18.63	52.1	5.56
	backward	19.63	44.87	6.43
	bi-directional	19.5	42.93	6.95

Table 1. Characteristics of pumping schemes for different signals for 470 mW of the pump power for forward pumping scheme, 454 mW of the pump power for backward pumping scheme, and 472 mW of the pump power for bi-directional pumping scheme.

The developed amplifier was studied using different pumping schemes with slightly different pump powers, and we would like to compare the power dependencies of gain and NF characteristics. As both the optical gain and noise figure have also a spectral dependence, we averaged the spectral magnitudes of these parameters in the range of 1400-1480 nm in order to compare an average performance of the pumping schemes. Such dependencies for forward, backward and bi-directional pumping scheme are presented in Fig. 12.

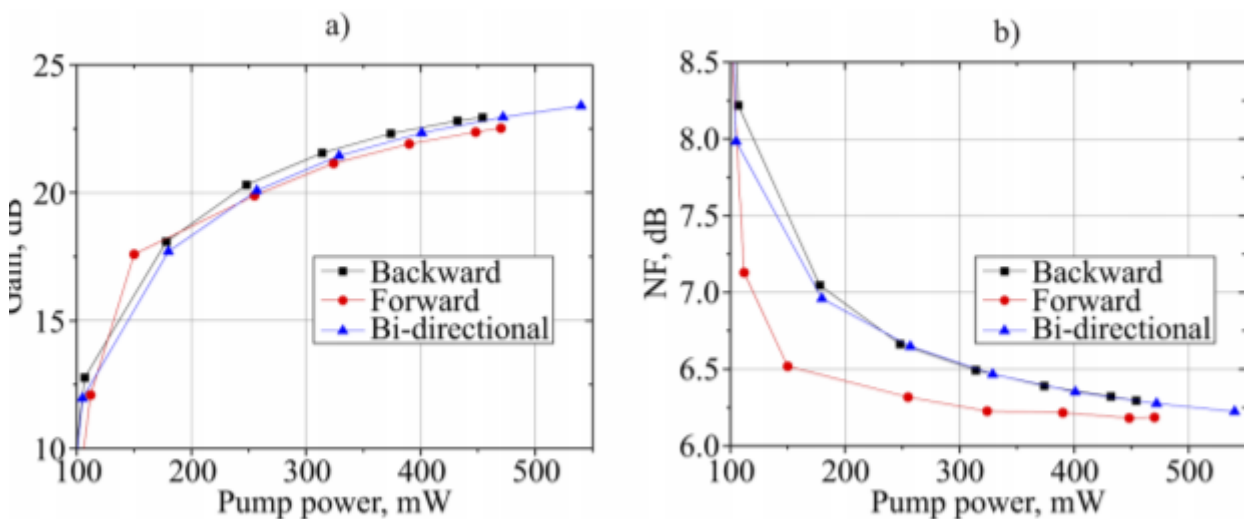


Fig. 12. Dependencies of the Gain (a) and NF (b) on the pump power

The graphs show that for almost all pump powers, the highest gain was achieved in the backward pumping scheme. The bi-directional pumping scheme showed intermediate gain magnitudes relatively to the backward and forward pumping schemes. The forward pumping scheme demonstrated a lower optical gain as compared to other pumping schemes. On the other hand, the lowest noise figure is achieved with the forward pumping scheme. The noise figure for bi-directional and backward pumping schemes is almost the same with slightly better performance in the bi-



directional scheme with pump powers less than 200 mW. Thus, the uniform pumping plays the crucial role for the amplifier performance in terms of the noise figure. It is worth noting that the NF for the forward pumping shows a noticeable saturation with pump power as compared to the bi-directional and backward pumping schemes. This indicates that a significant increase in the pump power for the bi-directional and backward pumping schemes will be comparable with the forward pumping NF. The same gain saturation was observed in the backward pumping scheme. Therefore, it is preferable to use the forward pumping scheme in order to achieve a moderate gain and an excellent noise performance with a relatively low pump power. Obviously, NF and gain characteristics should be nearly the same in all pumping schemes when the gain medium is well pumped.

### 4.3 Conclusion

A BDFA with maximum gain of 31 dB and minimum noise figure of 4.75 dB has been developed and studied in the forward, backward, and bi-directional pumping schemes. The demonstrated amplifier has a high gain (>20dB) in the whole spectral band of 1405-1460 nm. The three pumping schemes were compared in terms of the average noise figure, optical gain performance, and pump configuration. It was concluded that the forward pumping scheme is the most promising as excellent performance can be achieved at lower pump powers. However, it should be improved in terms of PCE, and the possible solutions are covered in the discussion. The high optical gain and the low NF of the BDFA operating in the E- and S-bands reported in this work with the overall BDFA performance comparable to the conventional EDFAs allows to consider BDFAs as a promising in-line amplifier with a potential to double the capacity of conventional C-band EDFA systems.

Further work is now underway to improve the modelling of this type of BDFA using machine learning techniques and to explore the performance of this amplifier in representative links over distances up to 160km.

## REFERENCES

1. Govind P Agrawal. Fiber-optic communication systems, volume 222. John Wiley & Sons, 2012.
2. Alessio Ferrari, Antonio Napoli, Johannes Karl Fischer, Nelson Manuel Simes da Costa, Andrea D'Amico, Joao Pedro, Wladek Forysiak, Erwan Pincemin, Andrew Lord, Alexandros Stavdas, et al. Assessment on the achievable throughput of multi-band it-t g. 652. d fiber transmission systems. *Journal of Lightwave Technology*, 2020.
3. T. Jiménez, V. López, F. Jiménez, O. González, and J.P. Fernández. Techno-economic analysis of transmission technologies in low aggregation rings of metropolitan networks. In *Optical Fiber Communication Conference*, page M2G.1. Optical Society of America, 2017.
4. RGH Van Uden, R Amezcua Correa, E Antonio Lopez, FM Huijskens, Cen Xia, G Li, A Schulzgen, H De Waardt, AMJ Koonen, and Chigo M Okonkwo. Ultra-high-density spatial division multiplexing with a few-mode multi-core fibre. *Nature Photonics*, 8(11):865–870, 2014.
5. Takayuki Kobayashi, Masanori Nakamura, Fukutaro Hamaoka, Kohki Shibahara, Takayuki Mizuno, Akihide Sano, H Kawakami, Akira Isoda, Munehiko Nagatani, H Yamazaki, et al. 1-pb/s (32 sdm/46 wdm/768 gb/s)-band dense sdm transmission over 205.6-km of single-mode heterogeneous multi-core fiber using 96-gbaudpdm-16qam channels. In *Optical Fiber Communication Conference*, pages Th5B–1. Optical Society of America, 2017.
6. René-Jean Essiambre, Gerhard Kramer, Peter J Winzer, Gerard J Foschini, and Bernhard Goebel. Capacity limits of optical fiber networks. *Journal of Lightwave Technology*, 28(4):662–701, 2010.
7. Peter J Winzer, David T Neilson, and Andrew R Chraplyvy. Fiber-optic transmission and networking: the previous 20 and the next 20 years. *Optics express*, 26(18):24190–24239, 2018.
8. M. Brierley, S. Carter, P. France, and J. Pedersen, “Amplification in the 1300 nm telecommunications window in aNd-doped fluoride fibre,” *Electron. Lett.*26, 329–330 (1990).
9. Y. Miyajima, T. Sugawa, and Y. Fukasaku, “38.2 db amplification at 1.31  $\mu$ m and possibility of 0.98  $\mu$ m pumping in Pr/sup 3+/-doped fluoride fibre,” *Electron. Lett.*27, 1706–1707 (1991).
10. S. Chen, Y. Jung, S.-u. Alam, D. J. Richardson, R. Sidharthan, D. Ho, S. Yoo, and J. M. Daniel, “Ultra-shortwavelength operation of thulium-doped fiber amplifiers and lasers,” *Opt. Express*27, 36699–36707 (2019).
11. L. Krzczanowicz, M. A. Z. Al-Khateeb, M. A. Iqbal, I. Phillips, P. Harper, and W. Forysiak, “Performance estimation of discrete Raman amplification within broadband optical networks,” in *Optical Fiber Communication Conference*, (Optical Society of America, 2019), pp. Tu3F–4.
12. J. W. Dawson, L. S. Kiani, P. H. Pax, G. S. Allen, D. R. Drachenberg, V. V. Khitrov, D. Chen, N. Schenkel, M. J. Cook, R. P. Cristet al., “E-band Nd 3+ amplifier based on wavelength selection in an all-solid micro-structured fiber,” *Opt. express*25, 6524–6538 (2017).
13. B. Pedersen, W. Miniscalco, and R. Quimby, “Optimization of Pr/sup 3+: Zblan fiber amplifiers,” *IEEE Photonicstechnology letters*4, 446–448 (1992).
14. B. B. Pedersen, W. J. Miniscalco, S. A. Zemon, and R. S. Quimby, “Analysis of Pr3+-and Nd3+-doped fiber amplifiers at 1300 nm,” in *Fiber Laser Sources and Amplifiers IV*, vol. 1789 (International Society for Optics and Photonics, 1993), pp. 191–200.
15. P. M. Krummrich, “Optimization of Pr3+-doped fiber amplifier design for different pump wavelengths,” *Opt. communications*114, 453–457 (1995).

16. E. M. Dianov, V. Dvoyrin, V. M. Mashinsky, A. A. Umnikov, M. V. Yashkov, and A. N. Gur'yanov, "CW bismuth fibre laser," *Quantum Electron.* 35, 1083 (2005).
17. V. V. Dvoyrin, A. V. Kir'yanov, V. M. Mashinsky, O. I. Medvedkov, A. A. Umnikov, A. N. Guryanov, and E. M. Dianov, "Absorption, gain, and laser action in bismuth-doped aluminosilicate optical fibers," *IEEE journal quantum electronics* 46, 182–190 (2009).
18. V. Dvoyrin, V. Mashinsky, A. Umnikov, A. Guryanov, and E. Dianov, "Lasers and amplifiers based on telecommunication fibers doped with bismuth," *LPHYS'09* p. 646 (2009).
19. V. V. Dvoirin, V. Mashinskii, O. I. Medvedkov, A. A. Umnikov, A. N. Gur'yanov, and E. M. Dianov, "Bismuth-doped telecommunication fibres for lasers and amplifiers in the 1400–1500-nm region," *Quantum Electron.* 39, 583 (2009).
20. V. Dvoyrin, O. Medvedkov, V. Mashinsky, A. Umnikov, A. Guryanov, and E. Dianov, "Optical amplification in 1430–1495 nm range and laser action in Bi-doped fibers," *Opt. Express* 16, 16971–16976 (2008).
21. N. Thipparapu, Y. Wang, S. Wang, P. Barua, and J. Sahu, "Bi-doped silica-based fiber amplifier for O-band transmission," in *Asia Communications and Photonics Conference*, (Optical Society of America, 2019), pp. S3G–6.
22. V. Mashinsky and V. Dvoyrin, "Bismuth-doped fiber amplifiers: State of the art and future prospect," in *2009 IEEE LEOS Annual Meeting Conference Proceedings*, (IEEE, 2009), pp. 775–776.
23. E. Manuylovich, V. Dvoyrin, D. Pushkarev, I. Mazaeva, and S. Turitsyn, "4-channel bi-doped fibre amplifier," in *45th European Conference on Optical Communication (ECOC 2019)*, (IET, 2019), pp. 1–4.
24. M. Melkumov, V. Mikhailov, A. Hegai, K. Riumkin, P. Westbrook, D. Di Giovanni, and E. Dianov, "E-band data transmission over 80 km of non-zero dispersion fibre link using bismuth-doped fibre amplifier," *Electron. Lett.* 53, 1661–1663 (2017).
25. N. Thipparapu, Y. Wang, A. Umnikov, P. Barua, D. Richardson, and J. Sahu, "40 dB gain all fiber bismuth-doped amplifier operating in the O-band," *Opt. letters* 44, 2248–2251 (2019).
26. V. Dvoyrin, V. Mashinsky, and S. Turitsyn, "Bismuth-doped fiber amplifier operating in the spectrally adjacent to EDFA range of 1425–1500 nm," in *Optical Fiber Communication Conference*, (Optical Society of America, 2020), pp. W1C–5.
27. Y. Wang, N. K. Thipparapu, D. J. Richardson, and J. Sahu, "Broadband bismuth-doped fiber amplifier with a record 115-nm bandwidth in the O and E bands," in *Optical Fiber Communication Conference*, (Optical Society of America, 2020), pp. Th4B–1.
28. S. Okamoto, K. Horikoshi, F. Hamaoka, K. Minoguchi and A. Hirano, "5-band (O, E, S, C, and L) WDM Transmission with Wavelength Adaptive Modulation Format Allocation," *ECOC 2016*; 2016, pp. 1–3.
29. Clifford Headley and Govind P. Agrawal, *Raman amplification in fibre optical communication systems* (Elsevier Academic Press, 2005), Chap. 5.
30. M. Asif Iqbal, L. Krzczanowicz, I. Phillips, P. Harper, and W. Forysiak, "150nm SCL-band transmission through 70km SMF using ultra-wideband dual-stage discrete raman amplifier," *Opt. InfoBase Conf. Pap.*, vol. Part F174-OFC 2020, no. c, pp. 4–6, 2020, doi: 10.1364/OFC-2020-W3E.4.
31. Md Asif Iqbal\*, Lukasz Krzczanowicz, Ian D. Philips, Paul Harper and Wladek Forysiak, "Performance characterisation of ultra-wideband Raman amplifiers", " *ECOC 2019*; , pp. 1–4.

32. S. Liang et al., "Record Gain, Low Noise Figure, C+L Band Lumped Raman Amplifier," 2020 European Conference on Optical Communications (ECOC), 2020, pp. 1-4, doi: 10.1109/ECOC48923.2020.9333376.
33. J. Bromage, "Raman Amplification for Fiber Communications Systems," *J. Light. Technol.*, vol. 22, no. 1, pp. 79–93, 2004, doi: 10.1109/JLT.2003.822828.
34. X. Zhou, M. Birk, A. Room, and L. A. South, "100 nm broadband Raman amplification in NZ-DSF fiber with zero-dispersion wavelength around 1500 nm," vol. 1, pp. 3–5, 2004.
35. L. Grüner-Nielsen and Y. Qian, "Dispersion-Compensating Fibers for Raman Applications," in *Raman Amplifiers for Telecommunications 1*, Springer New York, 2007, pp. 161–189.
36. A. El-taher et al., "High Gain, Flattened, Discrete Raman Fiber Amplifier and its Transmission Performance," in *2017 Conference on Lasers and Electro-Optics Europe & European Quantum Electronics Conference (CLEO/Europe-EQEC)*, 2017, doi: 10.1109/CLEOE-EQEC.2017.8087052.
37. M. Takahashi, R. Sugizaki, J. Hiroishi, M. Tadakuma, Y. Taniguchi, and T. Yagi, "Low-Loss and Low-Dispersion-Slope Highly Nonlinear Fibers," vol. 23, no. 11, pp. 3615–3624, 2005.
38. M. A. Iqbal et al., "Impact of pump-signal overlap in S+C+L band discrete Raman amplifiers," *Opt. Express*, vol. 28, no. 12, p. 18440, 2020, doi: 10.1364/oe.392258.
39. M. A. Iqbal, M. A. Z. Al-Khateeb, L. Krzczanowicz, I. D. Phillips, P. Harper, and W. Forysiak, "Linear and Nonlinear Noise Characterisation of Dual Stage Broadband Discrete Raman Amplifiers," *J. Light. Technol.*, vol. 37, no. 14, pp. 3679–3688, 2019, doi: 10.1109/JLT.2019.2919429.
40. VV Dvoyrin, VM Mashinsky, LI Bulatov, IA Bufetov, AV Shubin, MA Melkumov, EF Kustov, EM Dianov, AA Umnikov, VF Khopin, et al. Bismuth-doped-glass optical fibers—a new active medium for lasers and amplifiers. *Optics letters*, 31(20):2966–2968, 2006.
41. I. A. Bufetov, M. A. Melkumov, S. V. Firstov, K. E. Riumkin, A. V. Shubin, V. F. Khopin, A. N. Guryanov, and E. M. Dianov, "Bi-doped optical fibers and fiber lasers," *IEEE J. Sel. Top. Quantum Electron.* 20, 111–125 (2014).
42. A. Donodin, V. Dvoyrin, E. Manuylovich, L. Krzczanowicz, W. Forysiak, M. Melkumov, V. Mashinsky, and S. Turitsyn, "Bismuth doped fibre amplifier operating in E- and S- optical bands," *Opt. Mater. Express* 11, 127-135 (2021)
43. S. Firstov, V. Khopin, I. Bufetov, E. Firstova, A. Guryanov, and E. Dianov, "Combined excitation-emission spectroscopy of bismuth active centers in optical fibers," *Opt. Express* 19(20), 19551–19561 (2011).
44. Baney, Douglas M., Philippe Gallion, and Rodney S. Tucker. "Theory and measurement techniques for the noise figure of optical amplifiers." *Optical fiber technology* 6.2 (2000): 122-154.